Eur. Phys. J. D (2014) 68: 150
DOI: 10.1140/epjd/e2014-50100-1

THE EUROPEAN PHYSICAL JOURNAL D

Regular Article

Electromagnetically induced transparency for a double Fano-profile system

Thuan Bui Dinh[1,2], Van Cao Long[1,3,a], Wiesław Leoński[1], and Jan Peřina Jr.[4]

[1] Quantum Optics and Engineering Division, Institute of Physics, University of Zielona Góra, Prof. Z. Szafrana 4a, 65-516 Zielona Góra, Poland
[2] Vinh University, 182 Le Duan Street, Vinh City, Vietnam
[3] Faculty of Physics, University of Warsaw, 00-681 Warsaw, 69 Hoża, Poland
[4] RCPTM, Joint Laboratory of Optics of Palacký University and Institute of Physics of AS CR, Faculty of Science, Palacký University, 17. listopadu 12, 77146 Olomouc, Czech Republic

Received 3 February 2014 / Received in final form 28 March 2014
Published online 23 June 2014

Abstract. A Λ-like model of atomic levels involving two auto-ionizing states is considered. The levels are irradiated by two external electromagnetic fields, a strong driving and a weak probing ones. The analytical formula for medium susceptibility shows an additional electromagnetically induced transparency window caused by the second auto-ionizing level. Characteristics of both transparency windows are analyzed depending on parameters of auto-ionizing levels and the external driving field. Manipulation of these characteristics seems to be very effective because of their large sensitivity with respect to the parameters involved in the problem. This manipulation becomes even more feasible when considered model is implemented in so-called laser-induced continuum structure.

1 Introduction

According to the well-known Feynman rule of quantum mechanics, various possible transmission paths from an initial to a final state of a given system are possible and add their probability amplitudes. This results in quantum interference effects that lie in the heart of quantum mechanics. However, interference phenomena are interesting not only for basic physics, they can also be conveniently exploited in the design of physical systems with predefined properties. This quantum engineering has been found useful, e.g., in nano-technologies or quantum-information technologies. One of the most interesting effects arising from quantum interference is electromagnetically induced transparency (EIT). In this phenomenon widely discussed in numerous papers, a propagating beam of electromagnetic radiation is effectively not affected by the interaction with a medium though the medium undergoes a certain complex quantum evolution. Considering EIT, optical properties of the medium are modified by a strong driving field such that the incident weak probe field is not absorbed during its passage through the medium. This was observed in various experimental configurations including those of early experimental as well as theoretical considerations described in [1–7]. EIT effects have been observed in three basic configurations containing three discrete atomic levels, namely Λ-, V-type and ladder configurations (for the ladder system [8] and Λ-model [9,10], sometimes extended *Lambda*-models involving more than two lower levels are referred to as "tripod" ones [11,12]).

Another kind of interference effects discussed in this paper is related to auto-ionization (AI) processes in which quantum interference paths including both discrete and continuum levels play the crucial role. AI systems have been considered in numerous papers starting from the seminal paper by Fano [13]. Models involving discrete levels located above a continuum threshold (AI levels) have been considered in numerous works in atom-laser physics [14–28] (*and the references quoted therein*). They have been devoted to various aspects of AI systems. These so-called Fano systems (and Fano-like systems) have also been considered in other physical situations. They were discussed, for instance in a context of nano-physics, metamaterials [29], for the description of quantum dots (see, e.g., in Refs. [30–32] and quite recently, noninteracting waveguide arrays [33]. They were also a subject of various review articles [34,35]). AI models have also been applied in the context of electromagnetic-wave propagation in atomic media [36–38], for the description of interactions in a group of two [39–44] or three [45] atomic systems. Even quantum entanglement phenomena have been discussed in these systems [46].

As both the AI effects and EIT phenomena originate in quantum interference, they have many properties in common. In particular, there occurs similarity between

[a] e-mail: caolongvanuz@gmail.com

the quantum interference effects considered in AI systems' photoelectron spectra and the interference leading to EIT. Already in the early models of electromagnetic pulses propagating through a medium with the continuum and AI states both types of the interference have been considered [36,37]. The model of a Λ-system with the upper state replaced by a flat continuum has been discussed first by van Enk et al. [47]. Later, it has been extended to the model with an AI state [48]. Several aspects of this model including AI resonances have been analyzed by Raczyński et al. [49]. In this paper, we enrich the model by considering the second AI level with arbitrary energy. This generalizes the model discussed in reference [50] that contains two AI levels of the same energy. As it has been emphasized in references [51–53], the presence of an arbitrary additional AI state results in new quantum interference phenomena occurring in long-time photoelectron spectra which are considered in a more realistic model, where the external electromagnetic field has the white noise component [54]. Among others, it can induce an additional EIT window which parameters are controlled by the transition to (from) AI states. As is has been emphasized in reference [55], in framework of a full quatized model of the laser fields, the mechanism of autoionization is essentially similar to that of so-called laser-induced continuum structure (LICS), so LICS can be interpreted as a laser-induced autoionizing-like resonance. The best experimental demonstration of LICS so far has be done by Halfmann et al. [56,57] in the system of helium atoms, when LICS in the flat photoionization of helium has been observed. Also in the system of helium atoms, the population transfer via a continuum has been demonstrated experimentally [58]. Then one can produce tunable resonances with adjustable widths. For example, the control of Fano parameter by a fourth discrete level in the framework of LICS in a tripod system coupled via a continuum has been analyzed in reference [59]. Therefore the phenomena discussed here can be analyzed in the context of LICS with a wide possibility of their manipulation by changing the parameters involved in the problem.

The paper is organized as follows. The model is developed in Section 2. Its physical behavior is discussed in Section 3. Section 4 brings summary. The evaluation of integrals needed for the model is contained in Appendix.

2 The model

The considered model extends the models discussed by Raczyński et al. [49] and Bui Dinh et al. [50]. In reference [49] the Λ-like model with a single AI level and a flat continuum coupled to two lower discrete states by an external laser field has been discussed. Here, instead of a single AI level, we consider two AI states $|a_1\rangle$ and $|a_2\rangle$ with energies E_1 and E_2, respectively. Moreover, these AI states are embedded in a flat continuum $|E\rangle$. All these states are coupled by two external fields: a weak probe field of frequency ω_p coupling a discrete level $|b\rangle$ to levels $|a_1\rangle$ and $|a_2\rangle$ and a relatively strong driving control field with frequency ω_c interacting with another level $|c\rangle$ (for the scheme of energy levels, see Fig. 1). Configurational interaction between the AI levels $|a_1\rangle$, $|a_2\rangle$ and the flat continuum $|E\rangle$ is characterized by operators $\hat{U}_1$ and $\hat{U}_2$, respectively. Such configuration of atomic levels constitutes a *double-Λ* system that behaves differently compared to the usual Λ system. For instance, an additional Fano zero in the long-time photoelectron spectrum [51–53] is found in this enlarged system. These zeros are present even for large values of *asymmetry Fano parameters*, which is unusual. We note that, in the usual Fano profiles, Fano zeros move to minus infinity as the asymmetry parameter becomes large.

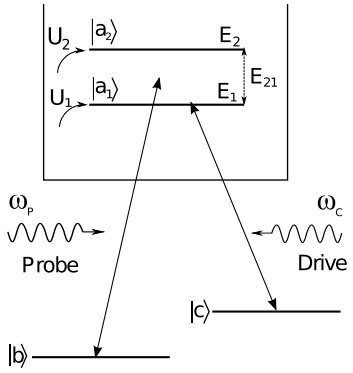

Fig. 1. Scheme of the model. Configuration coupling $\hat{U}_1$ ($\hat{U}_2$) between the AI level $|a_1\rangle$ ($|a_2\rangle$) and the flat continuum $|E\rangle$ gives the structured continuum $|E)$ in the form of a double Fano profile. The structured continuum $|E)$ is coupled to the level $|b\rangle$ ($|c\rangle$) by a weak probe (strong control) field of frequency ω_p (ω_c).

Coupling between atomic levels is mediated by external laser fields. The state $|b\rangle$ is coupled both to the continuum $|E\rangle$ and AI levels $|a_1\rangle$ and $|a_2\rangle$ by a weak probe field with amplitude ε_b. On the other hand, the state $|c\rangle$ communicates with the continuum $|E\rangle$ and AI levels $|a_1\rangle$ and $|a_2\rangle$ by a strong control field of amplitude ε_c. Obviously, non-resonant interactions with other levels lead to energy level shifts. Therefore, the field frequencies (especially, the frequency of strong driving field ω_c) should be chosen such that these shifts are taken into account.

Using the method of Fano diagonalization [13] we can replace all excited levels considered here by a structured continuum $|E)$. We note that this method was introduced by Fano [13] and developed later, for instance, in reference [60]. After Fano diagonalization, the discrete levels $|b\rangle$ and $|c\rangle$ are effectively coupled to a structured excited continuum with certain density of states that forms a *double Fano profile*. Its shape is determined by the following ratios between the matrix elements of the transitions from (to) a discrete level $|j\rangle$ to (from) the flat (or structured) continuum, $j = b, c$ [51]:

$$\frac{\langle j|\hat{d}|E)}{\langle j|\hat{d}|E\rangle} = \frac{(E-E_1)(E-E_2)+E(q_{1j}\gamma_1+q_{2j}\gamma_2)-(E_1q_{2j}\gamma_2+E_2q_{1j}\gamma_1)}{(E-E_1)(E-E_2)-iE(\gamma_1+\gamma_2)+i(E_1\gamma_2+E_2\gamma_1)}. \quad (1)$$

$$P^{+}(\omega_b) = N\int \langle b|\hat{d}|E\rangle\,\rho_{Eb}\,dE = -N\varepsilon_b\left(R_{bb} + \frac{\frac{1}{4}\varepsilon_2^2 R_{bc}R_{cb}}{E_b+\hbar\omega_b - E_c - \hbar\omega_c - i\hbar\gamma_{cb} - \frac{1}{4}\varepsilon_c^2 R_{cc}}\right) = \epsilon_0\,\varepsilon_b\,\chi(\omega_1) \tag{4}$$

$$\chi(\omega_b) = -\frac{N}{\epsilon_0}\left(R_{bb} + \frac{\frac{1}{4}\varepsilon_c^2 R_{bc}R_{cb}}{E_b+\hbar\omega_b - E_c - \hbar\omega_c - i\hbar\gamma_{cb} - \frac{1}{4}\varepsilon_c^2 R_{cc}}\right) \tag{5}$$

$$F_i(E) = \frac{(2E-E_1-E_2)^2 - E_{21}^2 + 2Q_i(2E-E_1-E_2) + 2E_{21}Q_{21i}}{(2E-E_1-E_-A_1)^2 + (\Gamma+A_2)^2}, \tag{8a}$$

$$F_j(E) = \frac{(2E-E_1-E_2)^2 - E_{21}^2 + 2Q_j(2E-E_1-E_2) + 2E_{21}Q_{21j}}{(2E-E_1-E_2+A_1)^2 + (\Gamma-A_2)^2} \tag{8b}$$

In this formula, the symbols $\gamma_1 = \pi|\langle a_1|U_1|E\rangle|^2$ and $\gamma_2 = \pi|\langle a_2|U_2|E\rangle|^2$ denote auto-ionization widths related to the presence of states $|a_1\rangle$ and $|a_2\rangle$, respectively. Similarly as in [51], we have introduced the *Fano asymmetry parameters* q_{1j} and q_{2j} in equation (1) for $j = b, c$:

$$q_{1j} = \frac{\langle j|\hat{d}|a_1\rangle}{\pi\langle j|\hat{d}|E\rangle\langle E|\hat{U}|a_1\rangle}, \tag{2a}$$

$$q_{2j} = \frac{\langle j|\hat{d}|a_2\rangle}{\pi\langle j|\hat{d}|E\rangle\langle E|\hat{U}|a_2\rangle}. \tag{2b}$$

A dipole-moment operator of electronic transitions is denoted as $\hat{d}$. According to their definitions, the Fano asymmetry parameters q_{1j} and q_{2j} give the ratios between the strengths of transition between two discrete levels and transition coming through the continuum state $|E\rangle$. If direct ionization is negligible, values of the q-parameters in (2) tend to infinity.

We assume that the energies of AI levels and the laser field frequencies are considerably higher than the energy threshold of the continuum. As a result, all threshold effects can be neglected and integrals over the energies can be extended to minus infinity. Moreover, all matrix elements corresponding to the transitions to (from) the flat continuum are assumed to depend only weekly on energy E. On the other hand, the matrix elements describing transitions to (from) the structured continuum with states $|E)$ (with a round brace]) depend strongly on energy parameter E.

The system described by its statistical operator $\hat{\rho}$ evolves according to the Liouville-von Neumann equation written in the *rotating wave approximation* (RWA) [61]. This approximation removes the terms oscillating fast in time and thus giving a negligible contribution. Applying the formalism of Fano diagonalization the following differential equations for the matrix elements of statistical operator $\rho_{Eb} = (E|\hat{\rho}|b\rangle$ and $\rho_{cb} = \langle c|\hat{\rho}|b\rangle$ are obtained:

$$i\,\hbar\dot{\rho}_{Eb} = (E - E_b - \hbar\omega_b)\,\rho_{Eb} - \frac{1}{2}\varepsilon_b\left(E|\hat{d}|b\right\rangle - \frac{1}{2}\varepsilon_c\left(E|\hat{d}|b\right\rangle\rho_{cb}, \tag{3a}$$

$$i\,\hbar\dot{\rho}_{cb} = (E + \hbar\omega_c - E_b - \hbar\omega_b - i\hbar\gamma_{cb})\,\rho_{cb} - \frac{1}{2}\varepsilon_c^*\int\langle c|\hat{d}|E)\rho_{Eb}dE. \tag{3b}$$

Similarly as in reference [49], we have introduced a phenomenological relaxation rate γ_{cb} for the coherence ρ_{cb}. We note that the derived equations are obtained in the first-order perturbation approximation in the probe-field amplitude ε_b.

Although the solution of differential equations (3) can be found for an arbitrary time t, we pay attention to only its long-time behavior. That is why, we derive the steady-state solution along the same vein as in reference [49]. We first express ρ_{cb} in terms of ρ_{Eb} to get an integral equation that is solved subsequently.

We need to reveal the component of polarization of the irradiated medium to study EIT. The positive-frequency component of polarization P^+ can be expressed as a function of the matrix element ρ_{Eb},

see equation (4) above.

In equation (4), N denotes the number of atoms and ϵ_0 stands for the vacuum permittivity. According to equation (4) the medium susceptibility χ attains the form [49]

see equation (5) above.

The parameters R_{ij} occurring in equations (4) and (5) are given as:

$$R_{ij}(\omega_b) = \lim_{\eta\to 0^+}\int\frac{\langle i|\hat{d}|E)(E|\hat{d}|j\rangle}{E_b - E + \hbar\omega_b + i\eta}dE, \quad i,j = b,c. \tag{6}$$

The limit $\eta \to 0^+$ assumed in equation (6) assures non-negativity of the imaginary part of susceptibility χ. It should be noted that the function to be integrated contains the matrix elements giving transitions to (from) the structured continuum $|E)$. Since these elements depend on energy, we have to apply the explicit expression (1) to obtain the energy dependence of the integrand. This results in the formula

$$R_{ij}(\omega_b) = \lim_{\eta\to 0^+} D_i D_j^*\int\frac{F_i(E)F_j(E)}{E_b - E + \hbar\omega_b + i\eta}dE, \quad i,j = b,c, \tag{7}$$

where

see equation (8) above

$$R_{ij}(\omega) = -2i\pi D_i D_j^* \left\{ \frac{\left[\left(\omega - \frac{E_{21}}{2}\right)^2 - \frac{E_{21}^2}{4}\right]\left[\Gamma\left(\omega - \frac{E_{21}}{2}\right)(Q_i + Q_j)\right] + \Gamma^2\left(\omega - \frac{E_{21}}{2}\right)^2 (Q_i Q_j - 1)}{\left[\left(\omega - \frac{E_{21}}{2}\right)^2 + \left(\frac{\Gamma + A_2}{2}\right)^2\right]\left[\left(\omega - \frac{E_{21}}{2}\right)^2 + \left(\frac{\Gamma - A_2}{2}\right)^2\right]} \right.$$
$$\left. + \frac{1}{2} + \frac{\mathcal{E}_p\left(\mathcal{E}_p^2 - \frac{E_{21}^2}{4}\right)(Q_i + Q_j) + \Gamma\mathcal{E}_p^2(Q_i Q_j - 1)}{-i\left(\mathcal{E}_p - \omega + \frac{E_{21}}{2}\right)(\Gamma + A_2)A_2} + \frac{\mathcal{E}_m\left(\mathcal{E}_m^2 - \frac{E_{21}^2}{4}\right)(Q_i + Q_j) + \Gamma\mathcal{E}_m^2(Q_i Q_j - 1)}{i\left(\mathcal{E}_m - \omega + \frac{E_{21}}{2}\right)(\Gamma - A_2)A_2} \right\} \quad (12)$$

$$R_{ij}(\omega) = -2i\pi D_i D_j^* \left\{ \frac{\left[\left(\omega - \frac{E_{21}}{2}\right)^2 - \frac{E_{21}^2}{4}\right]\left[\Gamma\left(\omega - \frac{E_{21}}{2}\right)(Q_i + Q_j)\right] + \Gamma^2\left(\omega - \frac{E_{21}}{2}\right)^2 (Q_i Q_j - 1)}{\left[\left(\omega - \frac{E_{21}}{2} - \frac{A_1}{2}\right)^2 + \frac{\Gamma^2}{4}\right]\left[\left(\omega - \frac{E_{21}}{2} + \frac{A_1}{2}\right)^2 + \frac{\Gamma^2}{4}\right]} \right.$$
$$\left. + \frac{1}{2} + \frac{\mathcal{C}_p\left(\mathcal{C}_p^2 - \frac{E_{21}^2}{4}\right)(Q_i + Q_j) + \Gamma\mathcal{C}_p^2(Q_i Q_j - 1)}{i\left(\mathcal{C}_p - \omega + \frac{E_{21}}{2}\right)\left[\left(\mathcal{C}_p + \frac{A_1}{2}\right)^2 + \frac{\Gamma^2}{4}\right]} + \frac{\mathcal{C}_m\left(\mathcal{C}_m^2 - \frac{E_{21}^2}{4}\right)(Q_i + Q_j) + \Gamma\mathcal{C}_m^2(Q_i Q_j - 1)}{i\left(\mathcal{C}_m - \omega + \frac{E_{21}}{2}\right)\left[\left(\mathcal{C}_m - \frac{A_1}{2}\right)^2 + \frac{\Gamma^2}{4}\right]} \right\} \quad (14)$$

and

$$A_1 = \frac{1}{\sqrt{2}}\left\{ \left[\left(4E_{21}^2 - \Gamma^2\right)^2 + 16E_{21}^2\left(\gamma_2 - \gamma_1\right)^2\right]^{\frac{1}{2}} + 4E_{21}^2 - \Gamma^2 \right\}^{\frac{1}{2}}, \quad (9a)$$

$$A_2 = \frac{1}{\sqrt{2}}\left\{ \left[\left(4E_{21}^2 - \Gamma^2\right)^2 + 16E_{21}^2\left(\gamma_2 - \gamma_1\right)^2\right]^{\frac{1}{2}} - 4E_{21}^2 + \Gamma^2 \right\}^{\frac{1}{2}}. \quad (9b)$$

In equations (8) and (9) we have introduced energy separation $E_{21} = E_2 - E_1$ between two AI levels, effective asymmetry parameters Q_k and AI width Γ defined as:

$$Q_k = \frac{q_{1k}\gamma_1 + q_{2k}\gamma_2}{\Gamma}, \quad k = b, c, \quad (10a)$$

$$\Gamma = \gamma_1 + \gamma_2. \quad (10b)$$

Also the quantities Q_{21k},

$$Q_{21k} = \frac{q_{2k}\gamma_2 - q_{1k}\gamma_1}{\Gamma}, \quad k = b, c, \quad (11)$$

have been found useful in writing equations (8). Moreover, we denote the matrix elements of dipole-moment transitions $\langle i|\hat{d}|E\rangle$ by D_i.

As the threshold effects are neglected we can extend the integration limits for $R_{ij}(\omega_b)$ from minus to plus infinity and find an analytical solution both for $R_{ij}(\omega_b)$ and the medium susceptibility $\chi(\omega_b)$. The obtained formulas are complex and can be found in Appendix together with details of their derivation.

3 Results

The analytical solution for $R_{ij}(\omega_b)$ takes a simple form for special cases. If we assume identical parameters of two AI levels ($\gamma_1 = \gamma_2$, $q_{1j} = q_{2j}$ for $j = b, c$) and their energy levels close to each other ($E_{21} < \Gamma$), we have $A_1 = 0$ and $A_2 = \sqrt{\Gamma^2 - E_{21}^2}$. The solution for R_{ij} can then be expressed as:

see equation (12) above.

In equation (12) we have redefined parameter ω, $\omega = \hbar\omega_b + E_b - E_1$ and introduced the following energy-like parameters:

$$\mathcal{E}_{p\atop m} = \frac{\Gamma \pm A_2}{2}. \quad (13)$$

If we additionally assume energy degenerate AI levels ($E_1 = E_2$, then $A_1 = 0$, $A_2 = \Gamma$, $\mathcal{E}_p = i\Gamma$ and $\mathcal{E}_m = 0$) and the solution (12) reduces to that derived by Raczyński et al. [49]. In this case, we deal with only one effective AI level described by effective parameters Q_i and Γ (for details, see [50]).

If the difference of energies of two AI levels is sufficiently large ($E_{21} > \Gamma = \gamma_1 + \gamma_2$), we have $A_1 = \sqrt{E_{21}^2 - \Gamma^2}$ and $A_2 = 0$. Then the solution for R_{ij} can be expressed as:

see equation (14) above,

using the parameters

$$\mathcal{C}_{p\atop m} = \frac{\pm A_1 + i\Gamma}{2}. \quad (15)$$

As we want to compare the obtained results with those found in reference [49] we assume the same values of parameters of the investigated system, i.e. $\gamma = 10^{-9}$ a.u., atomic population $N = 0.33 \times 10^{12}$ cm^{-3}, $D_b = 2$ a.u., $D_c = 3$ a.u. Values of asymmetry parameters vary in the interval $\langle 10, 100\rangle$ and field amplitude ε_c increases from 10^{-9} to 10^{-6} a.u.

Assuming identical parameters describing AI levels ($\gamma_1 = \gamma_2$ and $q_{1j} = q_{2j}$ for $j = b, c$), $Q_b = Q_c = 10$, $\Gamma = 10^{-9}$ a.u., and $\varepsilon_c = 4 \times 10^{-7}$ a.u., we analyze the spectral dependence of medium susceptibility χ in Figure 2. There occurs one zero in the dependence of $\mathrm{Im}\{\chi\}$ considering the energy degenerate case ($E_{21} = 0$) in accord with the results in references [49,50]. If the parameters of two AI levels differ, an additional zero appears

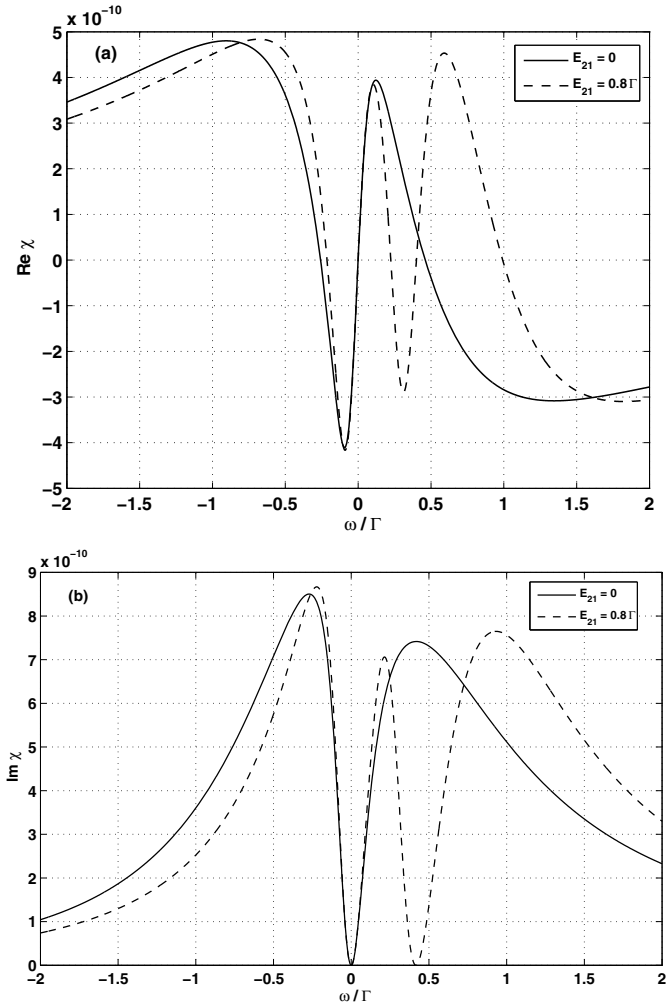

Fig. 2. Real (a) and imaginary (b) part of medium susceptibility χ depending on relative detuning ω/Γ; $\omega = \omega_b + (E_b - E_1)/\hbar$; $\varepsilon_c = 4 \times 10^{-7}$ a.u., $\Gamma = 10^{-9}$ a.u. and $Q_b = Q_c = 10$. Solid lines correspond to the degenerate case ($E_{21} = 0$), whereas dashed lines are appropriate to $E_{21} = 0.8\Gamma$.

in the dependence of Im$\{\chi\}$ indicating the occurrence of the second absorption window. Two absorption windows exist whenever either Q_{21k} parameters or energy levels of two AI levels differ. Also the second absorption window is characterized by normal dispersion (see Fig. 2b) resembling the behavior of long-time auto-ionization spectra for a system with two AI levels discussed in reference [51]. Also here, the consideration of the second AI state differing from the first one results in an additional Fano zero in these spectra. This similarity is not surprising as both effects originate in quantum interference between two ionization paths via the AI levels.

The strength of the driving field linearly proportional to Q_c influences the width of the EIT windows. The greater the strength, the wider the windows, as documented in Figure 3. To show how the strength of driving field (and hence, the value of Q_c) influences the widths of transparency windows, we present there the plots of both EIT windows' widths as a function of the asymmetry parameter Q_c, for the spectrally non-degenerate case ($E_{21} = 0.8\Gamma$). They are normalized to the width of the first transmission window for $Q_b = Q_c = 10$. We can see from Figure 3 that the width of the second window is equal to ∼4.8 and remains almost unchanged for the values of Q_c within the range from 1 to ∼17. Then, it increases slowly and reaches the value ∼6.5 for $Q_c = 40$. For the case of the first window, we observe more distinct changes of its width. For small values of Q_c ($Q_c \sim 1$) the window is very narrow, its width is very close to zero. With increasing values of the asymmetry parameter Q_c the width grows and reaches ∼9.3 for $Q_c = 40$. It is worth noting that this growth is almost linear for $Q_c \gtrsim 15$. Indeed, this window is considerably more influenced by the presence of additional quantum interferences than the second one due to the fact that the field is tuned exactly to the position of the lower AI level. Those facts suggest the strength of the driving field as a suitable parameter for tuning EIT effects.

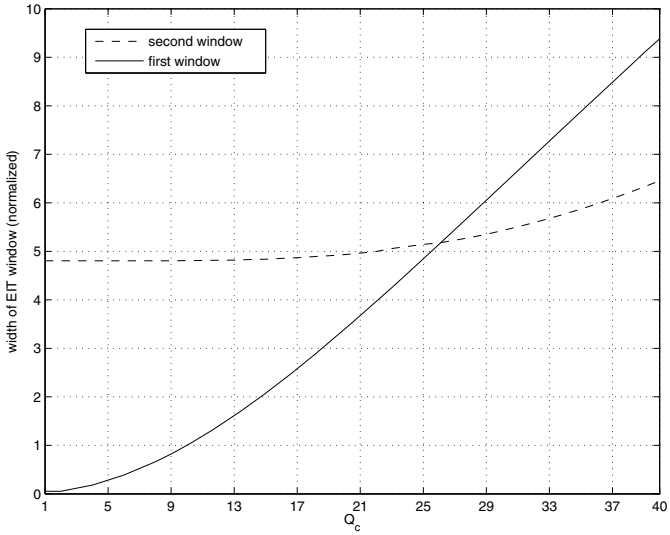

Fig. 3. Widths of two EIT windows as functions of the asymmetry parameter Q_c. All values are normalized to that for the first EIT window corresponding to the case $Q_b = 10$, $E_{21} = 0.8\Gamma$, $\Gamma = 10^{-9}$ a.u., $\varepsilon_c = 4 \times 10^{-7}$ a.u. and the remaining parameters are the same as those in the caption to Figure 2.

If we change the separation of energies E_{21} of two AI levels, the position of additional window changes according to the energy of the second AI level. We can see in Figure 4 that the larger the separation of energies, the more distant the second EIT window from the first one. Moreover, whereas the spectral width of the first window remains practically unchanged with the increasing values of E_{21}, the spectral width of the second window increases. The second EIT window even becomes broader than the first EIT window for sufficiently large values of the energy difference E_{21}. As Figure 5 documents, this width increases from zero to ∼4.2 as the distance between AI levels E_{21}/Γ changes from 0 (degenerate case) to 1.5. Moreover, if the level separation E_{21} equals ∼0.625, the both widths become the same.

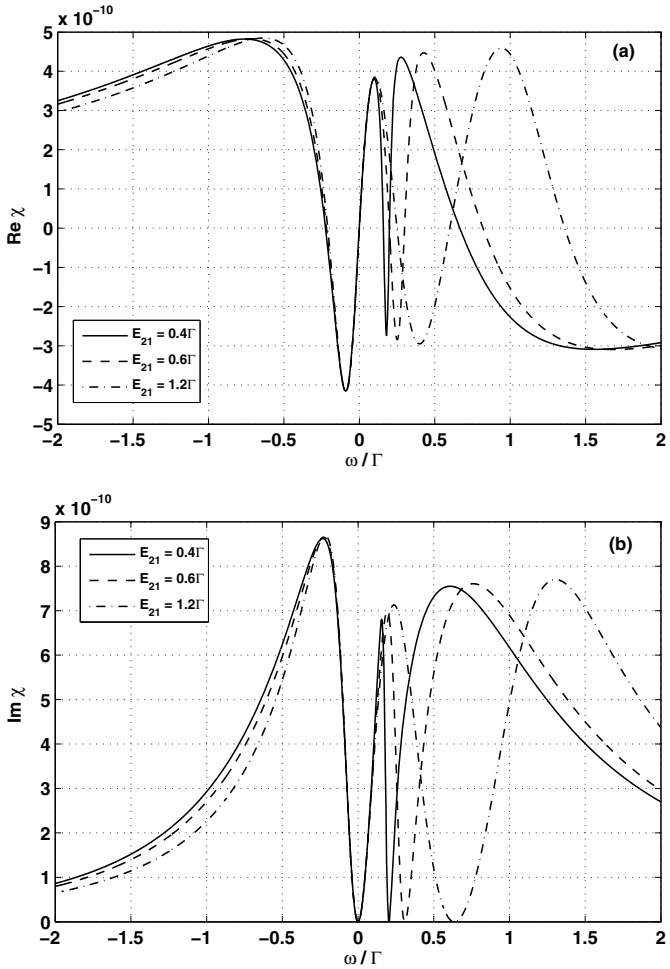

Fig. 4. Real (a) and imaginary (b) part of medium susceptibility χ as functions of relative detuning ω/Γ for various values of energy separation E_{21}. Values of the parameters are the same as those in the caption to Figure 2.

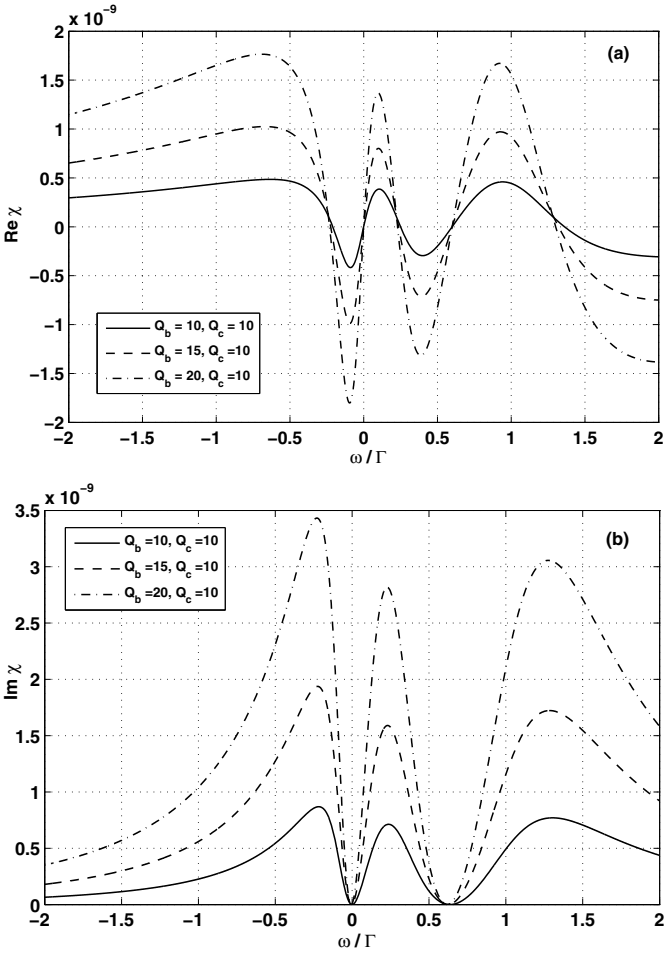

Fig. 6. Real (a) and imaginary (b) part of medium susceptibility χ depending on relative detuning ω/Γ. We assume AI energy levels separation $E_{21} = 1.2\Gamma$ and various values of Q_b. Moreover, $\varepsilon_c = 4\times10^{-7}$ a.u., $\Gamma = 10^{-9}$ a.u. Values of the other parameters are the same as those in the caption to Figure 2.

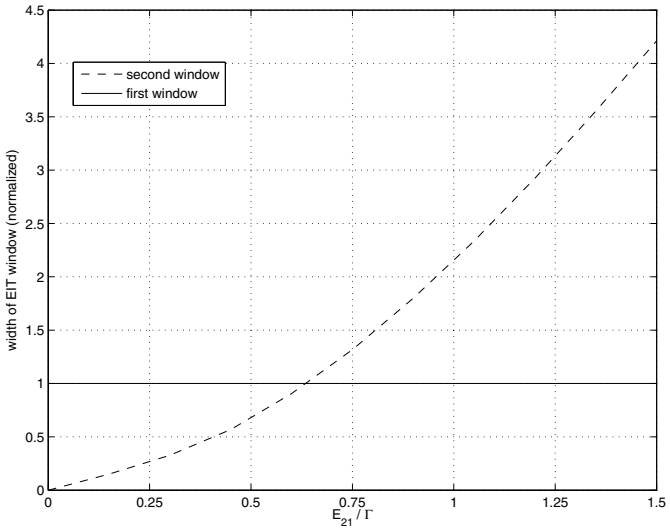

Fig. 5. Widths of two EIT windows as they depend on the level energy separations E_{21}; $Q_b = Q_c = 10$. Values of the other parameters are the same as in the caption to Figure 4.

Also the effective asymmetry parameter Q_b, linearly proportional to the probe field modifies the medium susceptibility χ. As shown in Figure 6, greater values of Q_b make EIT windows visible in the spectral dependence of $\mathrm{Im}\{\chi\}$ narrower. However, they keep the spectral positions of EIT windows unchanged. They also considerably increase variations in the dependence of $\mathrm{Re}\{\chi\}$, thus enhancing dispersion properties of the medium.

Parameters of the system thus allow for detailed tuning of EIT windows both in spectral position and width. The second EIT window opened by the second AI level is even more sensitive to the change of parameters and allows for wider windows. This is important in the pulsed propagation regime in which these spectral widths limit possible pulse durations from the point of view of EIT.

4 Summary

An analytical formula for medium susceptibility χ has been derived in the Λ-like system involving two general

AI levels. A second transparency window originating in the presence of the second AI level has been revealed. Its position and width depend on the values of parameters describing the interaction of levels with the driving field. Also the window's depth can be manipulated by changing the probe field. The appearance of the second transparency window occurs due to the quantum interference that dramatically modifies optical properties of the medium. Both discrete and continuum paths interfere together to form a complex response of the medium with two typical transparency windows. Especially the continuum paths have been found important for the observed effects. This has allowed to reveal an analogy between the observed effects and the phenomena occurring in the auto-ionization photoelectron spectra. The obtained results can be applied for tailoring the characteristics of electromagnetically-induced transparency in such media. Therefore, the multiple Fano resonance can be useful for slowing down of spectrally-broad light pulses. It is well-known that in framework of a full quantized model of the laser fields, the mechanism of autoionization is essentially the same to that of LICS, where LICS can be interpreted as a laser-induced autoionizing-like resonance. Therefore, the phenomena discussed here can be analyzed in the context of LICS with a wide possibility of their manipulation by changing the parameters involved in the problem.

J.P.Jr. acknowledges the support by Operational Program Research and Development for Innovations-European Regional Development Fund project CZ.1.05/2.1.00/03.0058 of MŠMT ČR.

Appendix

In Appendix, we derive an analytical formula for parameter R_{ij} given in equation (7) and needed for the determination of susceptibility χ by the residual method. In this method, we find the poles of the integrand in equation (8) inside the contour giving a physical solution (see, e.g., [15,51]).

We first discuss the case with $A_2 \neq \Gamma$ for which three poles are relevant,

$$E_{k0} = E_b + \hbar\omega_b + i\eta,$$
$$E_{k1} = \frac{E_1+E_2}{2} + \frac{A_1}{2} + i\frac{\Gamma+A_2}{2}, \quad \text{(A.1)}$$
$$E_{k2} = \frac{E_1+E_2}{2} - \frac{A_1}{2} + i\frac{\Gamma-A_2}{2} \quad \text{for} \quad A_2 < \Gamma,$$
$$E_{k2} = \frac{E_1+E_2}{2} - \frac{A_1}{2} - i\frac{\Gamma-A_2}{2} \quad \text{for} \quad A_2 > \Gamma. \quad \text{(A.2)}$$

Using these poles, the solution for R_{ij} attains the form

$$R_{ij}(\omega) = -i\pi D_i D_j^* (2[K_{ij0}(\omega) + K_{ij1}(\omega) + K_{ij2}(\omega) + K_{ij3}(\omega)] + 1), \quad i,j = b,c. \quad \text{(A.3)}$$

We note that $K_{ij2} = 0$ for $A_2 > \Gamma$ and $K_{ij3} = 0$ for $A_2 < \Gamma$. Otherwise, the parameters K_{ijn}, $n = 0,1,2,3$, can be expressed as:

$$\begin{aligned} K_{ij0}(\omega) = &\left\{ \left[\left(\omega - \frac{E_{21}}{2} - \frac{A_1}{2}\right)^2 + \left(\frac{\Gamma+A_2}{2}\right)^2 \right] \right. \\ &\times \left. \left[\left(\omega - \frac{E_{21}}{2} + \frac{A_1}{2}\right)^2 + \left(\frac{\Gamma-A_2}{2}\right)^2 \right] \right\}^{-1} \\ &\times \left\{ \left[\left(\omega - \frac{E_{21}}{2}\right)^2 - \frac{E_{21}^2}{4} \right] \left[\Gamma \left(\omega - \frac{E_{21}}{2}\right) \right. \right. \\ &\times (Q_b + Q_c) + \frac{\Gamma E_{21}}{2} (Q_{i21} + Q_{j21}) \left. \right] \\ &+ \Gamma^2 \left[\left(\omega - \frac{E_{21}}{2}\right) Q_i + \frac{E_{21}}{2} Q_{i21} \right] \\ &\times \left[\left(\omega - \frac{E_{21}}{2}\right) Q_j + \frac{E_{21}}{2} Q_{j21} \right] \\ &- \left. \left[\left(\omega - \frac{E_{21}}{2}\right) \Gamma + \frac{E_{21}}{2} (\gamma_2 - \gamma_1) \right]^2 \right\}, \quad \text{(A.4)} \end{aligned}$$

$$\begin{aligned} K_{ij1}(\omega) = &\left\{ i \left(E_{01} - \omega + \frac{E_{21}}{2}\right) (\Gamma + A_2) \right. \\ &\times \left. \left[\left(E_{01} + \frac{A_1}{2}\right)^2 + \left(\frac{\Gamma-A_2}{2}\right)^2 \right] \right\}^{-1} \\ &\times \left\{ \Gamma \left(E_{01}^2 - \frac{E_{21}^2}{4}\right) \right. \\ &\times \left[E_{01} (Q_i + Q_j) + \frac{E_{21}}{2} (Q_{i21} + Q_{j21}) \right] \\ &+ \Gamma^2 \left[E_{01} Q_i + \frac{E_{21}}{2} Q_{i21} \right] \left[E_{01} Q_j + \frac{E_{21}}{2} Q_{j21} \right] \\ &- \left. \left[E_{01}\Gamma + \frac{E_{21}}{2} (\gamma_2 - \gamma_1) \right]^2 \right\}, \quad \text{(A.5)} \end{aligned}$$

$$\begin{aligned} K_{ij2}(\omega) = &\left\{ i \left(E_{02} - \omega + \frac{E_{21}}{2}\right) (\Gamma - A_2) \right. \\ &\times \left. \left[\left(E_{02} - \frac{A_1}{2}\right)^2 + \left(\frac{\Gamma+A_2}{2}\right)^2 \right] \right\}^{-1} \\ &\times \left\{ \Gamma \left(E_{02}^2 - \frac{E_{21}^2}{4}\right) \right. \\ &\times \left[E_{02} (Q_i + Q_j) + \frac{E_{21}}{2} (Q_{i21} + Q_{j21}) \right] \\ &+ \Gamma^2 \left[E_{02} Q_i + \frac{E_{21}}{2} Q_{i21} \right] \left[E_{02} Q_j + \frac{E_{21}}{2} Q_{j21} \right] \\ &- \left. \left[E_{02}\Gamma + \frac{E_{21}}{2} (\gamma_2 - \gamma_1) \right]^2 \right\} \quad \text{(A.6)} \end{aligned}$$

$$K_{ij2}(\omega) = \left\{ \left(-\omega + \frac{E_{21}}{2} + E_{02}\right)^2 \left[\left(E_{02} - \frac{A_1}{2}\right)^2 + \Gamma^2\right]^2 \right\}^{-1} \left\{ \left[2\Gamma E_{02} \left[E_{02}(Q_i + Q_j) + \frac{E_{21}}{2}\left(Q_{i21} + Q_{j21}\right)\right] \right.\right.$$
$$+ \Gamma(Q_i + Q_j)\left(E_{02}^2 - \frac{E_{21}^2}{4}\right) + \Gamma^2 Q_i \left(E_{02}Q_j + \frac{E_{21}}{2}Q_{j21}\right) + \Gamma^2 Q_j \left(E_{02}Q_i + \frac{E_{21}}{2}Q_{i21}\right)$$
$$- 2\left[E_{02}\Gamma + \frac{E_{21}}{2}(\gamma_2 - \gamma_1)\right]\Gamma\left] \left(-\omega + \frac{E_{21}}{2} + E_{02}\right)\left[\left(E_{02} - \frac{A_1}{2}\right)^2 + \Gamma^2\right] - \left[\left(E_{02} - \frac{A_1}{2}\right)^2 + 1 + 2\left(E_{02} - \frac{A_1}{2}\right)\right.\right.$$
$$\times \left(-\omega + \frac{E_{21}}{2} + E_{02}\right)\left]\right] \left[\left(E_{02}^2 - \frac{E_{21}^2}{4}\right)\Gamma^2\left[E_{02}\left(Q_i + Q_j\right) + \frac{E_{21}}{2}\left(Q_{i21} + Q_{j21}\right)\right]\right.$$
$$\left.\left. + \Gamma^2\left[E_{02}Q_i + \frac{E_{21}}{2}Q_{i21}\right]\left[E_{02}Q_j + \frac{E_{21}}{2}Q_{j21}\right] - \left[E_{02}\Gamma + \frac{E_{21}}{2}(\gamma_2 - \gamma_1)\right]\right]\right\} \quad \text{(A.11)}$$

and

$$K_{ij3}(\omega) = \left\{ -i\left(E_{03} - \omega + \frac{E_{21}}{2}\right)(\Gamma - A_2) \right.$$
$$\times \left[\left(E_{03} - \frac{A_1}{2}\right)^2 + \left(\frac{\Gamma + A_2}{2}\right)^2\right]\Bigg\}^{-1}$$
$$\times \left\{ \Gamma\left(E_{03}^2 - \frac{E_{21}^2}{4}\right)\right.$$
$$\times \left[E_{03}\left(Q_i + Q_j\right) + \frac{E_{21}}{2}\left(Q_{i21} + Q_{j21}\right)\right]$$
$$+ \Gamma^2\left[E_{03}Q_i + \frac{E_{21}}{2}Q_{i21}\right]\left[E_{03}Q_j + \frac{E_{21}}{2}Q_{j21}\right]$$
$$\left. - \left[E_{03}\Gamma + \frac{E_{21}}{2}\left(\gamma_2 - \gamma_1\right)\right]^2\right\}. \quad \text{(A.7)}$$

In writing equations (A.4)–(A.7), we have redefined ω, $\omega = \hbar\omega_b + E_b - E_1$, and introduced energy-like parameters $E_{01} = [A_1 + i(\Gamma + A_2)]/2$, $E_{02} = -[A_1 + i(\Gamma - A_2)]/2$ and $E_{03} = -[A_1 - i(\Gamma - A_2)]/2$.

Provided that $A_2 = \Gamma$, we also consider three poles,

$$E_{k0} = E_b + \hbar\omega_b + i\eta,$$
$$E_{k1} = \frac{E_1 + E_2}{2} + \frac{A_1}{2} + i\Gamma, \quad \text{(A.8)}$$
$$E_{k2} = \frac{E_1 + E_2}{2} - \frac{A_1}{2}. \quad \text{(A.9)}$$

Whereas the first two poles are simple, the third one is of the second order. Taking this into account, we arrive at the formula for R_{ij},

$$R_{ij}(\omega) = -i\pi D_i D_j^*(2[K_{ij0}(\omega) + K_{ij1}(\omega) + K_{ij2}(\omega)] + 1). \quad \text{(A.10)}$$

In equation (A.10), the parameters K_{ij0} and K_{ij1} are given in equations (A.4) and (A.5) assuming $A_2 = \Gamma$. The remaining parameter K_{ij2} is defined as

see equation (A.11) above;

$E_{02} = -A_1/2$ in this case.

References

1. A. Imamoğlu, S.E. Harris, Opt. Lett. **14**, 1344 (1989)
2. S.E. Harris, J.E. Field, A. Imamoğlu, Phys. Rev. Lett. **64**, 1107 (1990)
3. J.E. Field, K.H. Hahn, S.E. Harris, Phys. Rev. Lett. **67**, 3062 (1991)
4. K.J. Boller, A. Imamoğlu, S.E. Harris, Phys. Rev. Lett. **66**, 2593 (1991)
5. A. Imamoğlu, J.E. Field, S.E. Harris, Phys. Rev. Lett. **66**, 1154 (1991)
6. E. Paspalakis, P.L. Knight, J. Opt. B: Quantum. Semiclass. Opt. **4**, S372 (2002)
7. A. Raczyński, J. Zaremba, S. Zielińska-Kaniasty, M. Artoni, G.C.L. Rocca, J. Mod. Opt. **56**, 2348 (2009)
8. K. Kowalski, V. Cao Long, H. Nguyen Viet, S. Gateva, M. Głódź, J. Szonert, J. Non-Cryst. Solids **355**, 1295 (2009)
9. A. Żaba, V. Cao Long, M. Głódź, E. Paul-Kwiek, K. Kowalski, J. Szonert, D. Woźniak, S. Gateva, Ukr. J. Phys. Opt. **14**, 137 (2013)
10. A. Żaba, E. Paul-Kwiek, K. Kowalski, J. Szonert, D. Woźniak, S. Gateva, V. Cao Long, M. Głódź, Eur. Phys. J. Special Topics **222**, 2197 (2013)
11. K. Słowik, A. Raczyński, J. Zaremba, S. Zielińska-Kaniasty, M. Artoni, G.C.L. Rocca, J. Mod. Opt. **58**, 978 (2011)
12. K. Słowik, A. Raczyński, J. Zaremba, S. Zielińska-Kaniasty, Opt. Commun. **285**, 2392 (2012)
13. U. Fano, Phys. Rev. **124**, 1866 (1961)
14. W.H. Parkinson, E.M. Reeves, Proc. Roy. Soc. Lond. A **331**, 237 (1972)
15. K. Rzążewski, J.H. Eberly, Phys. Rev. Lett. **47**, 408 (1981)
16. G.S. Agarwal, S.L. Haan, J. Cooper, Phys. Rev. A **28**, 1154 (1983)
17. A. Raczyński, J. Zaremba, Phys. Rev. A **40**, 1843 (1989)
18. A. Raczyński, J. Zaremba, J. Phys. B **23**, 3105 (1990)
19. W. Leoński, V. Bužek, J. Mod. Opt. **37**, 1923 (1990)
20. L. Journel, B. Rouvellou, C. Cubaynes, J.M. Bizau, F.J. Wuilleumier, M. Richter, P. Sladeczek, K.-H. Selbmann, P. Zimmermann, H. Bergeron, J. Phys. IV **3**, 217 (1993)
21. W. Leoński, J. Opt. Soc. Am. B **10**, 244 (1993)
22. E. Paspalakis, P.L. Knight, J. Phys. B **31**, 2753 (1998)
23. E. Paspalakis, P.L. Knight, J. Mod. Opt. **46**, 623 (1999)
24. M. Lewenstein, K. Rzążewski, Phys. Rev. A **61**, 022105 (2000)

25. A. Zawadzka, R.S. Dygdala, A. Raczyński, J. Zaremba, J. Kobus, J. Phys. B **35**, 1801 (2002)
26. W.-C. Chu, C.D. Lin, Phys. Rev. A **82**, 053415 (2010)
27. J. Zhao, M. Lein, New J. Phys. **14**, 065003 (2012)
28. P.R. Sharapova, O.V. Tikhonova, Quantum Electron. **42**, 199 (2012)
29. K. Choudhary, S. Adhikari, A. Biswas, A. Ghosal, A.K. Bandyopadhyay, J. Opt. Soc. Am. B **29**, 2414 (2012)
30. P. Trocha, J. Barnaś, Phys. Rev. B **76**, 165432 (2007)
31. A. Ridolfo, O.D. Stefano, N. Fina, R. Saija, S. Savasta, Phys. Rev. Lett. **105**, 263601 (2010)
32. I.E. Dotan, J. Scheuer, Opt. Commun. **285**, 3475 (2012)
33. I. Bayal, B.K. Dutta, P. Panchadhyayee, P.K. Mahapatra, J. Opt. Soc. Am. B **30**, 3202 (2013)
34. B. Luk'yanchuk, N.I. Zheludev, S.A. Maier, N.J. Halas, P. Nordlander, H. Giessen, C.T. Chong, Nat. Mater. **9**, 707 (2010)
35. A.E. Miroshnichenko, S. Flach, Y.S. Kivshar, Rev. Mod. Phys. **82**, 2257 (2010)
36. E. Paspalakis, M. Protopapas, P.L. Knight, J. Phys. B **31**, 775 (1998)
37. E. Paspalakis, N.J. Kylstra, P.L. Knight, Phys. Rev. A **60**, 642 (1999)
38. T. Bui Dinh, K. Doan Quoc, V. Cao Long, K. Dinh Xuan, Eur. Phys. J. Special Topics **222**, 2233 (2013)
39. B. Najjari, A.B. Voitkiv, C. Mueller, Phys. Rev. Lett. **105**, 153002 (2010)
40. A.B. Voitkiv, B. Najjari, Phys. Rev. A **82**, 052708 (2010)
41. J. Peřina Jr., A. Lukš, W. Leoński, V. Peřinová, Phys. Rev. A **83**, 053416 (2011)
42. J. Peřina Jr., A. Lukš, W. Leoński, V. Peřinová, Phys. Rev. A **83**, 053430 (2011)
43. J. Peřina Jr., A. Lukš, V. Peřinová, W. Leoński, Opt. Express **19**, 17133 (2011)
44. J. Peřina Jr., A. Lukš, V. Peřinová, W. Leoński, J. Russ. Laser Res. **32**, 454 (2011)
45. B. Najjari, C. Mueller, A.B. Voitkiv, New J. Phys. **14**, 250 (2012)
46. A. Lukš, J. Peřina Jr., W. Leoński, V. Peřinová, Phys. Rev. A **85**, 012321 (2012)
47. S.J. van Enk, J. Zhang, P. Lambropoulos, Phys. Rev. A **50**, 2777 (1994)
48. S.J. van Enk, J. Zhang, P. Lambropoulos, Phys. Rev. A **50**, 3362 (1994)
49. A. Raczyński, M. Rzepecka, J. Zaremba, S. Zielińska-Kaniasty, Opt. Commun. **266**, 552 (2006)
50. T. Bui Dinh, W. Leoński, V. Cao Long, J. Peřina Jr., Opt. Appl. **43**, 471 (2013)
51. W. Leoński, R. Tanaś, S. Kielich, J. Opt. Soc. Am. B **4**, 72 (1987)
52. W. Leoński, R. Tanaś, J. Phys. B **21**, 2835 (1988)
53. W. Leoński, R. Tanaś, J. Phys. D **21**, S125 (1988)
54. K. Doan Quoc, V. Cao Long, W. Leoński, Phys. Scr. **86**, 045301 (2012)
55. P.L. Knight, M.A. Lauder, B.J. Dalton, Phys. Rep. **190**, 1 (1990)
56. T. Halfmann, L.P. Yatsenko, M. Shapiro, B.W. Shore, K. Bergmann, Phys. Rev. A **58**, R46 (1998)
57. L.P. Yatsenko, T. Halfmann, B.W. Shore, K. Bergmann, Phys. Rev. A **59**, 2926 (1999)
58. T. Peters, L.P. Yatsenko, T. Halfmann, Phys. Rev. Lett. **95**, 103601 (2005)
59. R.G. Unanyan, N.V. Vitanov, B.W. Shore, K. Bergmann, Phys. Rev. A **61**, 043408 (2000)
60. P. Durand, I. Paidarová, F.X. Gadéa, J. Phys. B **34**, 1953 (2001)
61. L. Allen, J.H. Eberly, *Optical Resonance and Two-Level Atoms* (Wiley, New York, 1975)